Full field of view super-resolution imaging based on two static gratings and white light illumination

Javier García,[1] Vicente Micó,[2] Dan Cojoc,[3] and Zeev Zalevsky[4,*]

[1]Departamento de Óptica, Universitat de Valencia, c/o Dr. Moliner, 50, 46100 Burjassot, Spain

[2]AIDO, Technological Institute of Optics, Colour and Imaging, c/o Nicolás Copérnico, 7–13 Parc Tecnològic, 46980 Paterna (Valencia), Spain

[3]CNR-National Institute for Matter Physics (INFM), Laboratorio Nazionale TASC, Italy

[4]School of Engineering, Bar-Ilan University, Ramat-Gan 52900, Israel

*Corresponding author: zalevsz@macs.biu.ac.il

Received 13 February 2008; revised 6 May 2008; accepted 9 May 2008; posted 13 May 2008 (Doc. ID 92688); published 2 June 2008

The usage of two static gratings for obtaining super-resolved imaging dates back to the work by Bachl and Lukosz in 1967. However, in their approach a severe reduction in the field of view was the necessary condition for improving the resolution. We present an approach based on two static gratings without sacrificing the field of view. The key idea for not paying with the field of view is to use white light illumination to average the ghost images obtained outside the region of interest since the positions of those images are wavelength dependent. Moreover, large magnification is achieved by using a commercial microscope objective instead of a test system with a unity magnification as presented in previous works. Because of the large magnification, the second grating has a low spatial period. This allows us to create an intermediate image and use a second imaging lens with low resolution capability while still obtaining an imaging quality as good as that provided by the first imaging lens. This is an important improvement in comparison with the original super-resolving method with two fixed gratings. © 2008 Optical Society of America

OCIS codes: 100.6640, 110.4850.

1. Introduction

Super-resolution is a technique for having high-quality imaging while using low-quality (in the sense of resolution) imaging lenses. It allows us to take advantage of the properties provided by the low numerical aperture (NA) lenses (long working distance, large field of view, and large depth of focus), while the final improved resolution is equivalent to a higher NA lens. The classic way to achieve the super-resolution effect is by using information theory [1–3] and a given a priori knowledge of the input object; by knowing that the object belongs to a certain class of objects, it is possible to encode spatial-frequency information regarding the object's spectrum into unused channels of the optical system in such a way that this encoded information can pass through the limited system's aperture. Because of this a super-resolved image (i.e., with enhanced spatial resolution) can be obtained using an appropriate decoding process for the additional information.

But to obtain such resolution improvement, we must pay with some other degree of freedom that is not used as an information carrier in the image formation. Typical payments [4,5] are made with the time domain [6–10], the wavelength domain [11,12], the restricted object shape [13], the limited intensity dynamic range [14], and polarization [15–17]. An interesting approach involving two static gratings was first presented by Lukosz [18,19] and later expanded and tested by other researchers [20–22]. The Lukosz method [18,19,23,24] places two static gratings in one of two possible configurations: one grating before

0003-6935/08/173080-08$15.00/0

the object and the other before the image or one grating between the object and the image and the other after the image plane. Then a super-resolved imaging is obtained while payment in the field of view is assumed. To have super-resolution the two fixed gratings create ghost images that limit the field of view around the region of interest. Except the reduction in the field of view, the concept is applicable in a simple way since the two gratings are static. However, the discussed system had a magnification of one [18,19], therefore it had one major problem; one of the two gratings is not positioned between the object and the image. This means that for the case of placing the first grating after the object, a second imaging lens is required to image the second grating (which is positioned after the intermediate image plane) on the output plane. To do that the second imaging lens must provide a resolution as high as the resolution one wished to extract, therefore the super-resolution performed to the first lens seems to not be very useful.

We present an interesting modification of the super-resolution approach with the two fixed gratings [18,19] that has two main novelties. First, instead of using a monochromatic light source, we use polychromatic illumination. Since the position of each ghost image is wavelength-dependent (due to the gratings), the various images are averaged and no limitation on a restricted field of view is required. This is a very important release in the restrictions of this approach. The payment will be done in the dynamic range required from the sensor. Second, the imaging system we constructed has a large magnification ratio, therefore the second grating is magnified to match the first grating. Because of the difference in the ratio between the magnification of the two parts of the proposed configuration (in the original configuration both parts of the system had equal magnification of unity), the spatial period of the second grating is also very large, and the addition of the second imaging lens to image it to the output plane does not require a high-resolution lens. Therefore, the gratings perform super-resolution only on the first imaging lens, and the setup is therefore much more effective.

The technique described in this paper is applicable to practical imaging systems since this is, to the best of our knowledge, the first paper that reports how to overcome the field of view limitation that was introduced 30 years ago in the static grating approach of Lukosz. This is a very practical innovation using the two static grating approach for practical configurations with improved resolving capabilities.

In Section 2 we briefly present the theoretical analysis of the presented approach. In Section 3 we show some experimental results. Section 4 concludes the paper.

2. Mathematical Analysis

In this section we will prove that indeed when a polychromatic illumination is used instead of a monochromatic one, the approach of two fixed gratings can provide super-resolved imaging without paying with the field of view. The trade-off in this case will be the dynamic range since the undesired replications will be averaged into a uniform intensity distribution. (Because the various replications do not fall on the same spatial position, their summation is the equivalent of the spatial averaging of the product between the image of the object and the spectral distribution of the illumination. Such an averaging approximately yields a constant in case of a large number of spatially dispersed replications.) Figure 1 shows the sketch of the optical setup we propose. The setup includes two cascaded imaging modules. The first has a magnification of $M_1 = u_1/v_1$ and the second of $M_2 = u_2/v_2$. The fixed gratings, G1 and G2, are positioned at distances of z_0 and z_1 from the input and the intermediate image planes, respectively. The focal lengths of the two imaging lenses are F_1 and F_2, respectively. The values of v_1, u_1, and F_1 as well as v_2, u_2, and F_2 fulfil the imaging relation. Each of the two imaging lenses has a finite aperture determining its limits of spatial resolution.

In the two fixed gratings approach, the first grating is used as an encoding function (that encodes the spatial information of the input object and allows its transmission through the band-limited aperture of the imaging lens), while the second is used as a decoder (that reconstructs the encoded information and produces the super-resolved image). Both must have identical spatial distributions except for a scaling factor that depends on the ratio between the magnifications of the two parts of the optical configuration of Fig. 1. We intend to use a large ratio between M_2 and M_1 such that the spatial period of the required grating G2 will be very large and will not be deformed by the cut off frequency of the imaging lens of the second part of the configuration of Fig. 1.

Since we aim to prove the effect of using polychromatic illumination, due to reasons of simplicity for the mathematical validation, we will assume that $M_1 = M_2 = 1$, i.e., $v_1 = u_1 = 2F_1$, $v_2 = u_2 = 2F_2$, and $F_1 = F_2 = F$. We refer to Ref. [24] for the mathematical derivation. There an optical setup with similar assumptions to ours is mathematically analyzed. The analysis is based on basic Fourier optics relations, while the outline for the formulation is as follows: The input field distribution is free space propagated a distance of z_0 and multiplied by the first grating G1. Then it is virtually propagated backwards by a free space distance of $-z_0$ to reflect the effect of this grating over the input plane. The result is Fourier trans-

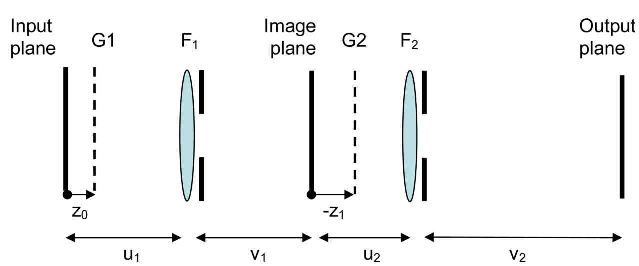

Fig. 1. (Color online) Proposed experimental setup.

formed and multiplied by a rectangular function $\mathrm{rect}(\Delta\mu/\lambda 2\mathrm{F})$, where $\Delta\mu$ represents the lateral extent of the aperture of the imaging lens. The result is inverse Fourier transformed to reach the image plane. The distribution there is free space propagated a distance of $-z_1$ and multiplied by the grating G2, then propagated backwards a free space distance of z_1 to reflect the grating to the image plane, which is imaged with a magnification of 1 (in the simplified assumption) to the output plane. The field distribution obtained in the image or in the output plane, after all those mathematical procedures, equals

$$u_0(x, z = 4\mathrm{F}) = \sum_m \sum_n A_m B_n \int_{-\infty;}^{\infty;} \tilde{u}_0(\nu) \mathrm{rect}\left(\frac{\nu + m\nu_0}{\Delta\mu/\lambda 2\mathrm{F}}\right) \cdot \exp\left[2\pi i \left(x(m\nu_0 + n\nu_1) + \nu(z_0\lambda m\nu_0 - z_1\lambda n\nu_1) + \frac{z_0\lambda m^2\nu_0^2}{2} - \frac{z_1\lambda n^2\nu_1^2}{2} - z_1\lambda mn\nu_0\nu_1\right)\right] \exp[2\pi i x\nu]\mathrm{d}\nu, \tag{1}$$

where v_0 and v_1 are the fundamental frequencies of the gratings G1 and G2, respectively; A_m and B_n are the Fourier series coefficients of G1 and G2, respectively; $\tilde{u}_0(\nu)$ is the Fourier transform of the high-resolution input field distribution; n and m are integers; λ is the optical wavelength; and v is the spectral coordinate. In this simplified configuration the axial location of $z = 4\mathrm{F}$ is the position of the image plane, which is basically also the output plane since the effect of the grating G2 that appears after the image plane was already taken into account (i.e., reflected to the output plane).

The physical meaning of Eq. (1) can be explained as follows: basically it is an inverse Fourier transform of the Fourier of the input field distribution $\tilde{u}_0(\nu)$ multiplied by a synthetic aperture and an additional phase term. Because of the summation over the index m, the spectrum of the input field $\tilde{u}_0(\nu)$ is actually multiplied by a synthetic aperture that is wider than the original aperture set by the dimensions of the imaging lens. The rect expression is synthetically enlarged due to its replications and following the summation over the index m. Therefore, since more spatial frequencies can pass through (since we have extended the synthetic aperture), the output image can contain spatial resolution equal to the one confined within the input field distribution. However, Eq. (1) also contains an undesired phase term of

$$\exp\left[2\pi i \left(x(m\nu_0 + n\nu_1) + \nu(z_0\lambda m\nu_0 - z_1\lambda n\nu_1) + \frac{z_0\lambda m^2\nu_0^2}{2} - \frac{z_1\lambda n^2\nu_1^2}{2} - z_1\lambda mn\nu_0\nu_1\right)\right].$$

To have true super-resolution we need to see in which conditions this term becomes a constant that does not affect the inverse Fourier transform integral. We chose $z_0 = -z_1$ and $\nu_0 = \nu_1 = \frac{\Delta\mu}{\lambda 2\mathrm{F}}$ (two identical gratings), which yield

$$u_0(x, z = 4\mathrm{F}) = \sum_m \sum_n A_m B_n \int_{-\infty;}^{\infty;} \tilde{u}_0(\nu) \times \mathrm{rect}\left(\frac{\nu + m\nu_0}{\Delta\mu/\lambda 2\mathrm{F}}\right) \cdot \exp\left[2\pi i \left(x(\nu + \nu_0(m+n)) + \nu(z_0\lambda(m+n)\nu_0) + \frac{z_0\lambda\nu_0^2}{2}(m+n)^2\right)\right]\mathrm{d}\nu. \tag{2}$$

Note that the values of z_0 and z_1 are measured according to the notations of Fig. 1. This means that choosing $z_0 = -z_1$ means that either G1 and G2 are in front of the input and image planes, respectively, or the both are after those planes. For $n = -m$ super-resolution is obtained since

$$u_0(x, z = 4\mathrm{F}) = \int_{-\infty;}^{\infty;} \tilde{u}_0(\nu)\left[\sum_m A_m B_{-m} \mathrm{rect}\left(\frac{\nu + m\nu_0}{\Delta\mu/\lambda 2\mathrm{F}}\right)\right] \times \exp[2\pi i x\nu]\mathrm{d}\nu. \tag{3}$$

The expression in Eq. (3) is the proof of super-resolution since the spectrum of the input field distribution $\tilde{u}_0(\nu)$ is multiplied by an extended synthetic aperture (the term in brackets) allowing the transmission of higher spatial frequencies and therefore reconstruction of the output field $u_0(x, z = 4\mathrm{F})$ containing smaller spatial details.

Choosing $m = -n$ is equal to paying with the field of view since all the replicas that do not fulfil this condition (crossed terms with $n \neq -m$) will appear at spatial positions of

$$x_{m,n} = \lambda z_0 \nu_0 (m+n). \tag{4}$$

The field of view for the input field distribution should be smaller than the expression of Eq. (4) such that the undesired terms for which $m \neq -n$ will not distort the reconstructed image of the output plane.

This derivation has been done before and is described in Refs. [18,19,24]. Now we will see how the use of polychromatic illumination can remove the drawback of this approach related to the payment with the field of view.

Note that Eq. (3) is for the field distribution. In our case, since we illuminate with polychromatic illumination, we will compute the intensity for the final outcome of the mathematical derivation, then average it for the various wavelengths because a monochromatic detector averages the readout over the spectral range of the illumination:

$$|h(x,z=4\mathrm{F})|^2 = \int_{\Delta\lambda} S(\lambda) \sum_m \sum_n \sum_{m'} \sum_{n'} A_m B_n A^*_{m'} B^*_{n'}$$
$$\times \int_{-\infty;}^{\infty;} \int_{-\infty;}^{\infty;} \mathrm{rect}\left(\frac{\nu + m\nu_0}{\Delta\mu/\lambda 2\mathrm{F}}\right) \mathrm{rect}\left(\frac{\nu' + m'\nu_0}{\Delta\mu/\lambda 2\mathrm{F}}\right)$$
$$\cdot \exp\left[2\pi i\left(x(\nu + \nu_0(m+n)) + \nu(z_0\lambda(m+n)\nu_0)\right.\right.$$
$$\left.\left. + \frac{z_0\lambda\nu_0^2}{2}(m+n)^2\right)\right] \cdot \exp\left[-2\pi i\left(x(\nu' + \nu_0(m'+n'))\right.\right.$$
$$\left.\left. + \nu'(z_0\lambda(m'+n')\nu_0) + \frac{z_0\lambda\nu_0^2}{2}(m'+n')^2\right)\right] \mathrm{d}\lambda \mathrm{d}\nu d\nu', \tag{5}$$

where $|h|^2$ is the intensity impulse response for the spatially incoherent case, $\Delta\lambda$ is the spectral range of the illuminating source (over which we performed our averaging), and $S(\lambda)$ is the spectral distribution of the source. We will assume that this distribution is more or less uniform within the spectral range of $\Delta\lambda$. To obtain the expression for the impulse response, we have assumed that in the input plane we have a point source, i.e., its Fourier transform is a constant: $\tilde{u}_0(\nu) = 1$. To compute the output distribution in case any general distribution is positioned in the input plane, we need to convolve this impulse response with the intensity of the input object. We denote

$$\xi \triangleq \nu(z_0(m+n)\nu_0) + \frac{z_0\nu_0^2}{2}(m+n)^2 - \nu'(z_0(m'+n')\nu_0)$$
$$- \frac{z_0\nu_0^2}{2}(m'+n')^2.$$

Inspecting the obtained result within the spatial spectral range of the synthetic super-resolved aperture leads to

$$|h(x,z=4\mathrm{F})|^2 = \sum_m \sum_n \sum_{m'} \sum_{n'} A_m B_n A^*_{m'} B^*_{n'}$$
$$\times \int_{-\infty;}^{\infty;} \int_{-\infty;}^{\infty;} \mathrm{rect}\left(\frac{\nu + m\nu_0}{\Delta\mu/\bar{\lambda} 2\mathrm{F}}\right) \mathrm{rect}\left(\frac{\nu' + m'\nu_0}{\Delta\mu/\bar{\lambda} 2\mathrm{F}}\right)$$
$$\cdot \exp[2\pi i x(\nu + \nu_0(m+n) - \nu' - \nu_0(m'+n'))]$$
$$\cdot \int_{\Delta\lambda} S(\lambda) \exp[2\pi i\lambda\xi] \mathrm{d}\lambda \mathrm{d}\nu \mathrm{d}\nu', \tag{6}$$

where $\bar{\lambda}$ is the average wavelength of the illuminating spectral band.

Since we assume the spectral bandwidth of the illumination to be wide enough and uniform enough, we can approximate that

$$\int_{\Delta\lambda} S(\lambda) \exp[2\pi i\lambda\xi] \mathrm{d}\lambda \approx S(\bar{\lambda}) \int_{\Delta\lambda} \exp[2\pi i\lambda\xi] \mathrm{d}\lambda = \kappa \cdot \delta(\xi), \tag{7}$$

where κ is a constant. Since Eq. (7) contains a delta function, it is valid only for $\xi = 0$, which is obtained only for the case when the integer indexes fulfil $m = -n$ and $m' = -n'$. This is true since only then the phase of the exponent $\exp(2\pi i\lambda\xi)$ is zero, and therefore all the components are added constructively during the integration process over the full range of values of λ. Therefore the result of Eq. (3), having the physical meaning of super-resolved imaging, may be obtained without limiting the field of view:

$$|h(x,z=4\mathrm{F})|^2 = \left| \int_{-\infty;}^{\infty;} \left[\sum_m A_m B_{-m} \mathrm{rect}\left(\frac{\nu + m\nu_0}{\Delta\mu/\bar{\lambda} 2\mathrm{F}}\right)\right] \times \exp(2\pi i x\nu) \mathrm{d}\nu \right|^2. \tag{8}$$

The proposed super-resolving technique, allowing us to improve the resolution with two fixed gratings without paying in the field of view, still requires the payment in the dynamic range or the signal-to-noise ratio (SNR) in the detector. Averaging over the wavelengths eventually reduces the SNR of the information. Nevertheless, since detectors with a high dynamic range of 12 bits or more are commonly available, it is easier to pay with the dynamic range and allow its partial sacrifice than the previous payment in the field of view, which was much more limiting.

3. Experimental Results

To demonstrate the presented approach, the optical setup shown in Fig. 2 was constructed in the laboratory. The experimental setup included two imaging modules. The magnification of the first imaging system was selected to be 7.5×. The second imaging module magnifies the first image plane into the output plane, and its magnification can be selected according to our benefit. As a first imaging system, we used a long working distance infinity corrected Mitutoyo microscope lens with a 0.14 NA. A photographic objective with a variable focus (or magnification) is used as the second imaging system. Notice that similar to commercial microscopes, the second imaging system acts as a tube lens. This lens should not have the restriction of having a fixed magnification.

White light illumination is provided by a halogen lamp source, and a 3CCD color video camera (SONY Model DXC-950P) captures the final images. The halogen lamp has a relatively uniform spectrum in the visible range (it resembles blackbody radiation), and therefore the assumption for the spectral uniformity, as done in the mathematical analysis of Section 2, is valid. The spectrum of the halogen lamp is presented in Fig. 3(a). These data were taken from the literature. In Fig. 3(b) we show the sensitivity response of the three channels (R, G, and B) of the CCD. Those charts are important since what is relevant to the operation principle is not the illuminating spectrum alone but rather its product with the sensitivity of the detector. In Fig. 3(c) we plot the combined result of the camera sensitivity and the spectrum of the illumination by adding the three channels' sensitiv-

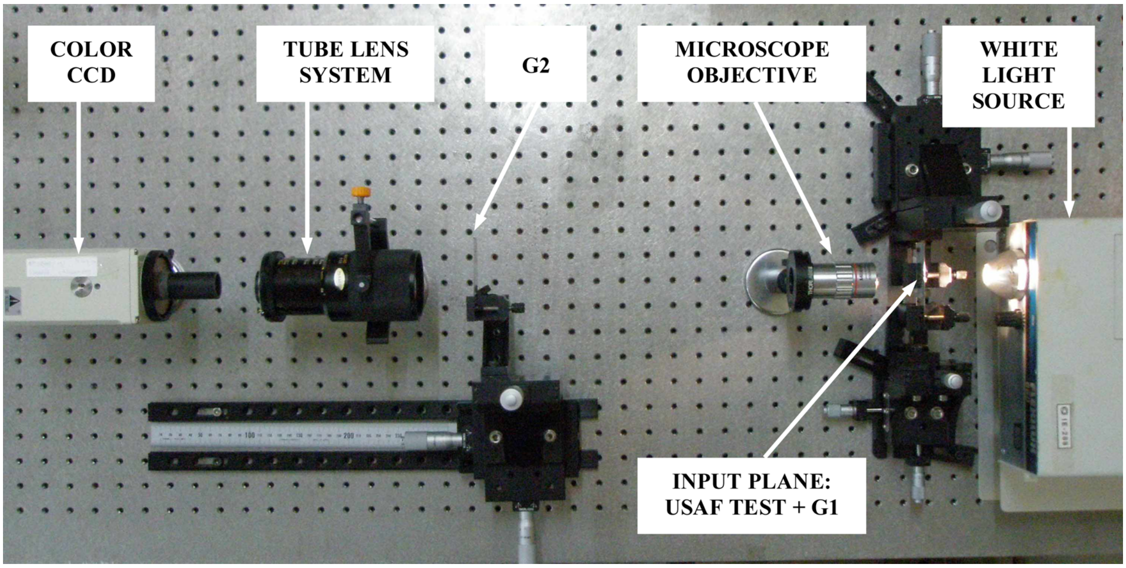

Fig. 2. (Color online) Photograph of the experimental setup in the laboratory.

ities, each one multiplied by the spectrum irradiance. To demonstrate the validity of our assumption, for the delta function of Eq. (7), we computed the magnitude of the Fourier transform of the chart of Fig. 3(c). The display is in decibel units. As can be seen in Fig. 3(d), the magnitude of the Fourier is in-

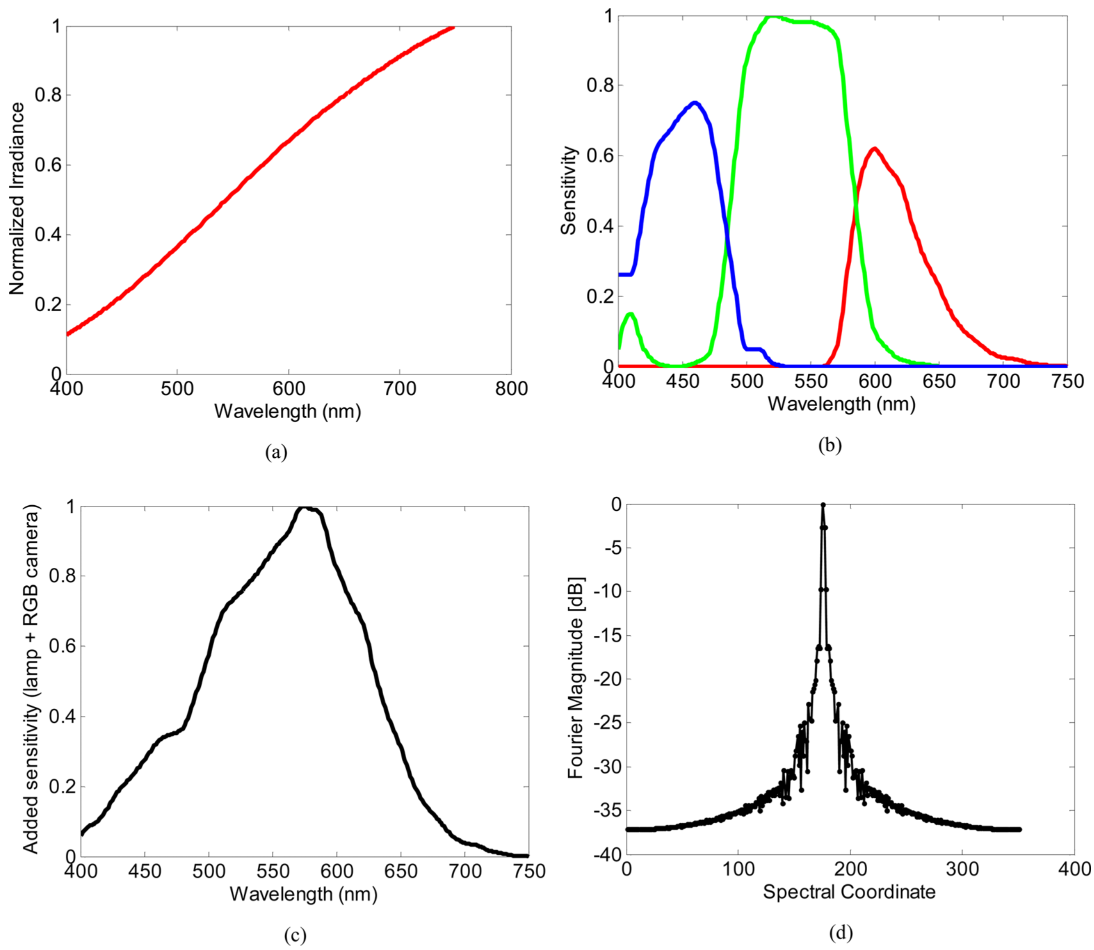

Fig. 3. (a) Illumination spectrum of the halogen lamp. (b) Sensitivity response of the three channels (R, G, and B) of the CCD. (c) The combined response of the illumination spectrum and the sensitivity of the CCD (the addition of the three channels' sensitivities each multiplied by the spectral irradiance of the lamp). (d) The magnitude of the Fourier transform of the combined chart of (c).

deed nearly a delta function with an attenuation of more than 10 times for the values surrounding the peak of the delta.

Two precision Ronchi ruling slides were used as diffraction gratings in the experiment. The period of both the G1 and G2 gratings was $p_1 = 600\,\mathrm{lp/mm}$ and $p_2 = 80\,\mathrm{lp/mm}$, respectively (due to the ratio of magnifications between the two parts of our setup, the second grating could be a low-frequency grating). The period of the first grating is selected depending on the NA of the microscope lens that was used as the first imaging system. To achieve a resolution gain factor close to 2, the diffraction angle for a central wavelength of the broadband spectral light used as illumination must be nearly twice the angle defined by the NA of the objective. This means a period of $\sim 500\,\mathrm{lp/mm}$ is suitable for such a resolution improvement. Once the first grating is selected, we can both fix the magnification of the microscope objective and properly select the G2 grating, or the opposite. In our case a ratio of 7.5 was defined by the periods of both diffraction gratings, and this will be the magnification that will be aimed for the microscope lens.

Since the second imaging setup had a magnification such that the low NA of the imaging lenses did not reduce resolution any more, a true super-resolved image was obtained. The experiment was performed for one-dimensional (1D) super-resolution, and therefore the super-resolving factor obtained may be easily extracted just by comparing the resulting resolution on both principal axes. Our purpose was to demonstrate the super-resolution and show that the result is obtained without paying with the field of view when the white light source is used.

We have used a negative high-resolution U.S. Air Force test target. Figure 4(a) depicts the full field of view image when the presented approach is used and the magnification of the second imaging system is near to 1. We can see that because the ghost images are wavelength sensitive due to the diffraction orders of the gratings, they are averaged in the background (which means there is no limitation on the field of view). On the other hand the proper combination of diffraction orders between both gratings compensates their chromatic dispersion and reinforces the white light super-resolved image. In Fig. 4(b) we show the classic Bachl and Lukosz [19] monochromatic experiment by simply placing an interference filter (515 nm main wavelength) before the input plane. Because the ghost images are not averaged, the final resolution is limited by the distance between the replicated diffraction orders. In this case a reduction in the field of view is needed to allow super-resolution over the region of interest.

In Fig. 4(c) we show the cross section of the region marked by the square in Fig. 4(a). The purpose was to compute the reduction in contrast due to the usage of white light illumination. The cross section was computed in two locations [as indicated in the upper right-hand corner of Fig. 4(c)]. The circles (in red) indicate the cross section in the lower part of the marked region where no replication was generated and thus no reduction in contrast. The squares (in blue) show the cross section in the upper part of the marked region where the various replications

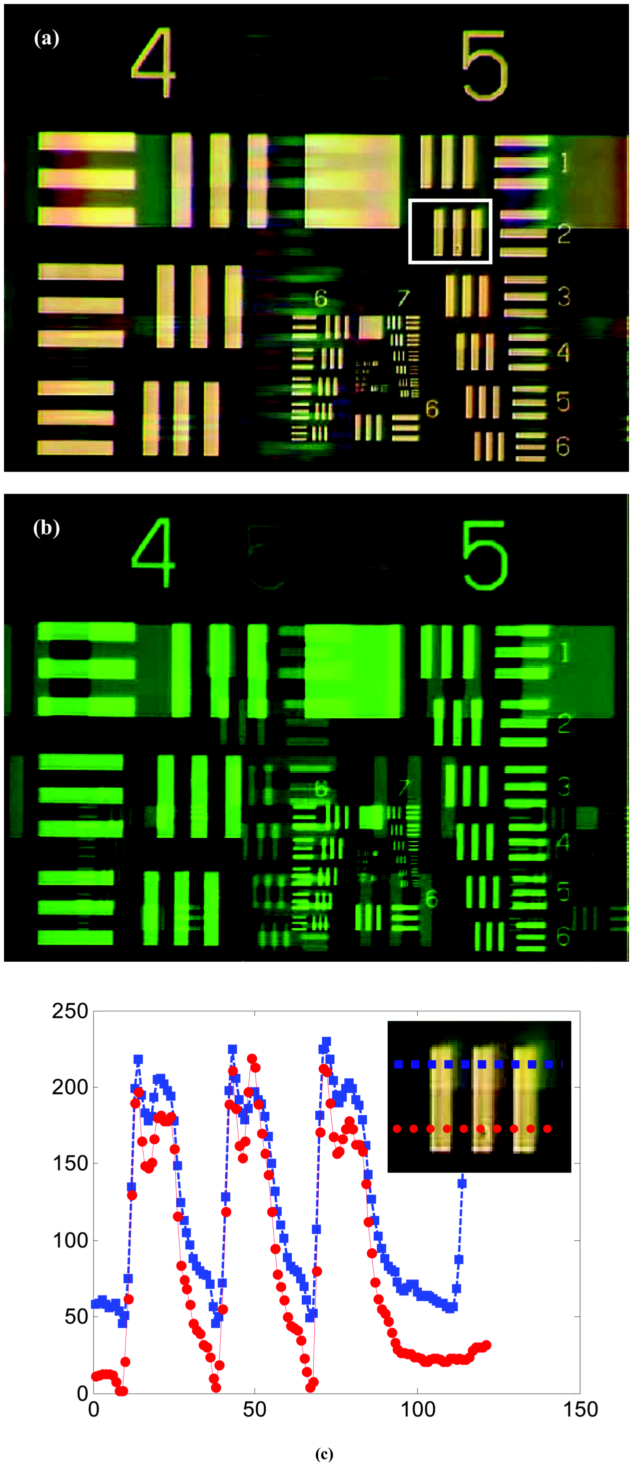

Fig. 4. Experimental results. (a) The full field of view super-resolved image obtained using the presented approach, and (b) the full field of view image with monochromatic illumination (Bachl and Lukosz [19] approach). (c) Cross section of (a) for the purpose of computing the reduction in contrast.

(differently positioned due to the use of the polychromatic illumination) reduced the contrast of the bars. The contrast of the circles is 0.946 while that of the squares is 0.586. This reduction of 39% in contrast is due to the replications. Our computation of contrast was performed according to

$$C = \frac{I_{\max} - I_{\min}}{I_{\max} + I_{\min}}, \tag{9}$$

where $I_{\max}$ is the maximal value of the intensity and $I_{\min}$ is its minimal value.

Note that this super-resolution approach, as other approaches involving gratings, is not energetically efficient. Because of the gratings only a certain portion of the input energy arrives at the region of interest in the output plane. However, one must distinguish between energetic efficiency and contrast. The reduction in energy may be compensated if the illumination source is strong enough and if the detector has an automatic gain control function that adapts the dynamic range of its sampling (analog to digital conversion) to the average level of the arriving energy. The contrast reduction cannot be compensated in the hardware since it is related to the SNR and to the number of sampling bits identifying the signal from the background noises.

Theoretically speaking, the reduction in contrast can be estimated as follows: since the contrast is defined as formulated in Eq. (9) and, due to the replications, a DC background is added to the intensity ($I_{\max}$ and $I_{\min}$), one may obtain the expression for new contrast as

$$C = \frac{I_{\max} - I_{\min}}{I_{\max} + I_{\min} + 2\mathrm{DC}}, \tag{10}$$

where the DC background is exactly the average of the imaged object:

$$\mathrm{DC} = \frac{\int_{\Delta\lambda} S(\lambda) u_0(x - \beta_1\lambda, y - \beta_2\lambda)\mathrm{d}\lambda}{\Delta\lambda}, \tag{11}$$

where β_1 and β_2 are constants and u_0 is the imaged object. For instance, in the case that resembles our experiment where the object has an average gray level, i.e., DC of 60, and in spatial region where $I_{\max} = 180$ and $I_{\min} = 5$, one will obtain a contrast reduced to 0.58.

In Fig. 5 we shown the central part of the resolution target where a magnification of close to 7× is chosen for the tube lens system. One may see that indeed the resolution of the vertical lines (Group 9, Element 2 corresponding with 575 lp/mm) is much higher than the resolution of the horizontal lines (Group 8, Element 4 corresponding with 362 lp/mm). Therefore the experiment has demonstrated resolution improvement by a factor of almost 2.

4. Conclusions

We have presented an applicable practical modification over the basic approach presented by Lukosz in Ref. [18] and experimentally demonstrated later in Ref. [19]. Unlike these previous works, in the presented approach the super-resolved image is obtained without paying with the field of view due to the usage of white light illumination. Experimental results validate the presented approach in which both encoding and decoding gratings are positioned between the object and the image planes, and the required position for both gratings is obtained using the proper magnification for the imaging setup. Although the super-resolution effect presented here is 1D, a two-dimensional (2D) case can be easily

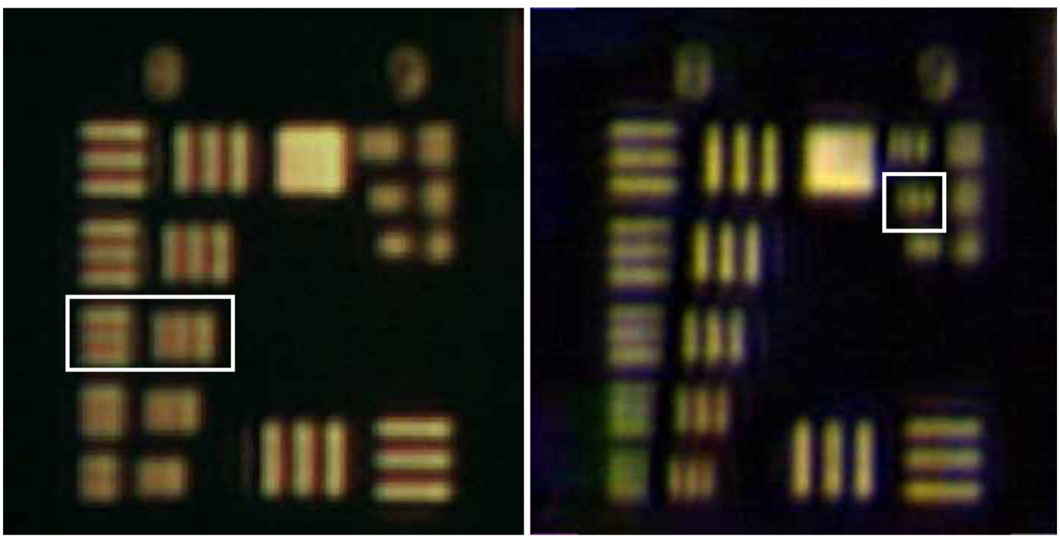

(a) (b)

Fig. 5. (Color online) Experimental results; the high-resolution region of interest in Fig. 4(a). The squares in vertical and horizontal lines mark the resolution limit with and without applying the presented approach, respectively.

obtained by simply replacing the 1D gratings with 2D gratings.

The super-resolved imaging, which is obtained with two fixed gratings and without paying with the field of view, causes a reduction in the SNR of the spatial information. Nevertheless, since detectors with a high dynamic range of 12 bits or more are commonly available, it is easier to pay with the dynamic range and to allow its partial sacrifice than it is to pay with the field of view, which is much more crucial.

In the experimental verification we have demonstrated super-resolving factor of 2 without payment in the field of view.

This work was supported by the Spanish Ministerio de Educación y Ciencia under the project FIS2007-60626.

References

1. G. Toraldo di Francia, "Resolving power and information," J. Opt. Soc. Am. **45**, 497–501 (1955).
2. G. Toraldo di Francia, "Degrees of freedom of an image," J. Opt. Soc. Am. **59**, 799–804 (1969).
3. J. Cox and J. R. Sheppard, "Information capacity and resolution in an optical system," J. Opt. Soc. Am. A **3**, 1152–1158 (1986).
4. A. W. Lohmann, R. G. Dorsch, D. Mendlovic, Z. Zalevsky, and C. Ferreira, "About the space bandwidth product of optical signal and systems," J. Opt. Soc. Am. A **13**, 470–473 (1996).
5. Z. Zalevsky, D. Mendlovic, and A. W. Lohmann, "Understanding super resolution in Wigner space," J. Opt. Soc. Am. A **17**, 2422–2430 (2000).
6. M. Francon, "Amélioration the résolution d'optique," Il Nuovo Cimento Suppl. **9**, 283–290 (1952).
7. W. Lukosz, "Optical systems with resolving powers exceeding the classical limits II," J. Opt. Soc. Am. **57**, 932–941 (1967).
8. A. Shemer, D. Mendlovic, Z. Zalevsky, J. García, and P. García-Martínez, "Superresolving optical system with time multiplexing and computer decoding," Appl. Opt. **38**, 7245–7251 (1999).
9. Z. Zalevsky, J. García, P. García-Martínez, and C. Ferreira, "Spatial information transmission using orthogonal mutual coherence coding," Opt. Lett. **30**, 2837–2839 (2005).
10. D. Mendlovic, I. Kiryuschev, Z. Zalevsky, A. W. Lohmann, and D. Farkas, "Two dimensional super resolution optical system for temporally restricted objects," Appl. Opt. **36**, 6687–6691 (1997).
11. A. I. Kartashev, "Optical systems with enhanced resolving power," Opt. Spectrosc. **9**, 204–206 (1960).
12. D. Mendlovic, J. Garcia, Z. Zalevsky, E. Marom, D. Mas, C. Ferreira, and A. W. Lohmann, "Wavelength multiplexing system for a single mode image transmission," Appl. Opt. **36**, 8474–8480 (1997).
13. M. A. Grimm and A. W. Lohmann, "Superresolution image for one-dimensional object," J. Opt. Soc. Am. **56**, 1151–1156 (1966).
14. Z. Zalevsky, P. García-Martínez, and J. García, "Superresolution using gray level coding," Opt. Express **14**, 5178–5182 (2006).
15. W. Gartner and A. W. Lohmann, "An experiment going beyond Abbe's limit of diffraction," Z. Phys. **174**, 18 (1963).
16. A. W. Lohmann and D. P. Paris, "Superresolution for nonbirefringent objects," Appl. Opt. **3**, 1037–1043 (1964).
17. A. Zlotnik, Z. Zalevsky, and E. Marom, "Superresolution with nonorthogonal polarization coding," Appl. Opt. **44**, 3705–3715 (2005).
18. W. Lukosz, "Optical systems with resolving powers exceeding the classical limits," J. Opt. Soc. Am. **56**, 1463–1472 (1966).
19. A. Bachl and W. Lukosz, "Experiments on superresolution imaging of a reduced object field," J. Opt. Soc. Am. **57**, 163–169 (1967).
20. E. Sabo, Z. Zalevsky, D. Mendlovic, N. Konforti, and I. Kiryuschev, "Super resolution optical system using two fixed generalized Dammann gratings," Appl. Opt. **39**, 5318–5325 (2000).
21. Z. Zalevsky, D. Mendlovic, and A. W. Lohmann, "Super resolution optical systems using fixed gratings," Opt. Commun. **163**, 79–85 (1999).
22. E. Sabo, Z. Zalevsky, D. Mendlovic, N. Konforti, and I. Kiryuschev, "Super resolution optical system using there fixed generalized gratings: Experimental results," J. Opt. Soc. Am. A **18**, 514–520 (2001).
23. Z. Zalevsky, D. Mendlovic, and A. W. Lohmann, "Optical system with improved resolving power," in *Progress in Optics* (Elsevier, 1999), Vol. **60**, Chap. 4.
24. Z. Zalevsky and D. Mendlovic, *Optical Super Resolution* (Springer-Verlag, 2003).